

Hadronic b decays to open charm and a measurement of the CKM angle γ

V.V. Gligorov, CERN

On behalf of the LHCb collaboration

25th February 2013



Overview

Today I will discuss two topics

1) Searches for suppressed modes and measurements of branching fractions in B decays to open charm

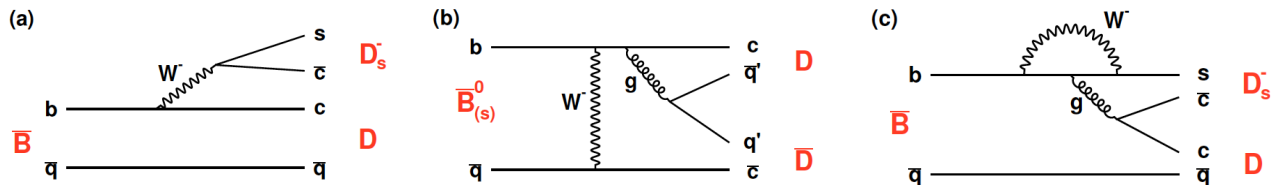
=> Explores the sizes of decay diagrams (tree/penguin/exchange/etc.) contributing to B decays and the importance of rescattering, which are key inputs for understanding CPV measurements.

2) A combined LHCb measurement of the CKM angle γ with 1fb^{-1} of data

=> Includes inputs from ADS, GLW, and GGSZ analyses

b hadron decays to
open charm

Studies of double charm B decays



A rich collection of decay modes and diagrams

CP violation in these modes is sensitive to $B_{(s)}$ mixing phases, γ , $\Delta\Gamma_s$

Suppressed modes mediated by W-exchange diagrams and suppressed penguin diagrams, and their branching fractions can help us to understand these processes better.

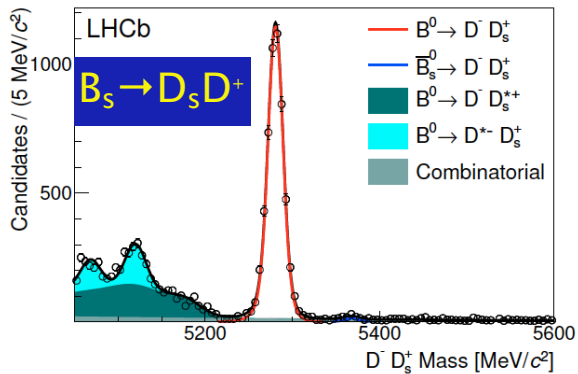
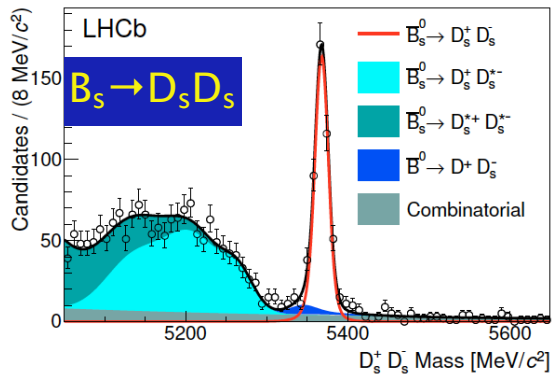
Common selection : $D^0 \rightarrow K\pi/K3\pi$, $D^+ \rightarrow K\pi\pi$, $D_s \rightarrow KK\pi$

Arbitration between the different D mesons using RICH information.

Decision tree for D-from-B signature trained on real data $B \rightarrow D\pi$ decays.

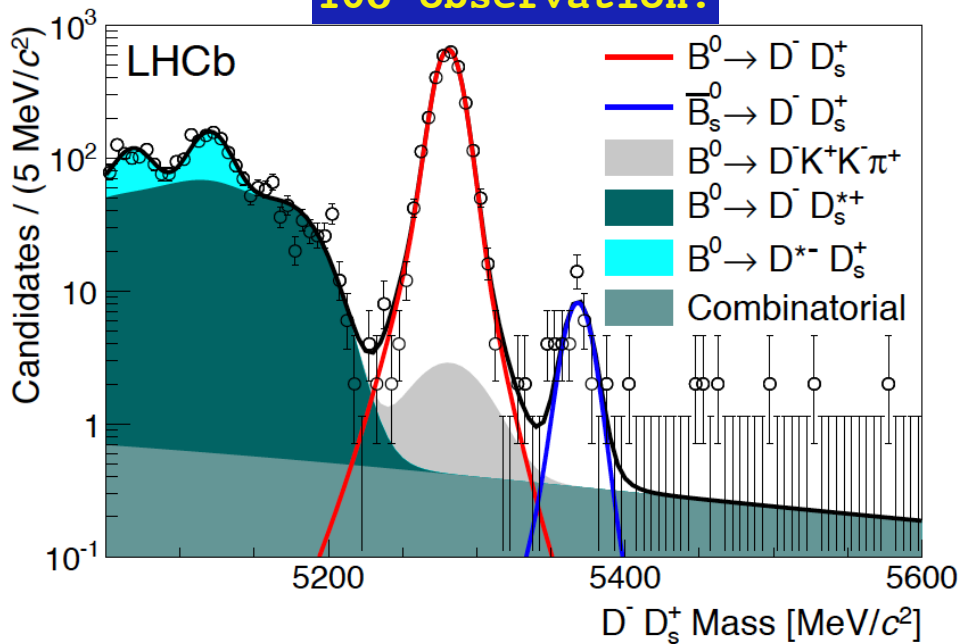
Charmless decays are suppressed by requiring that the D vertex is separated from the B vertex.

$$B_s \rightarrow D_s D_s$$

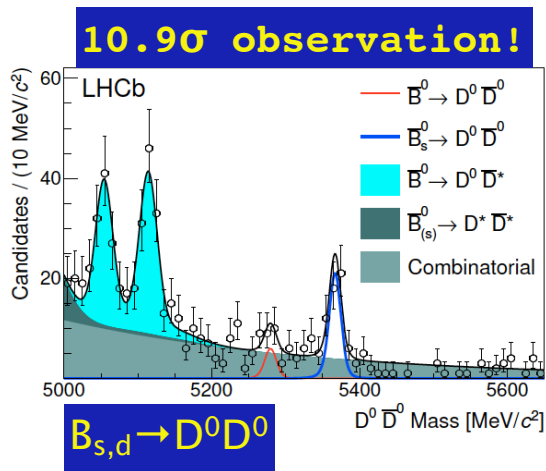
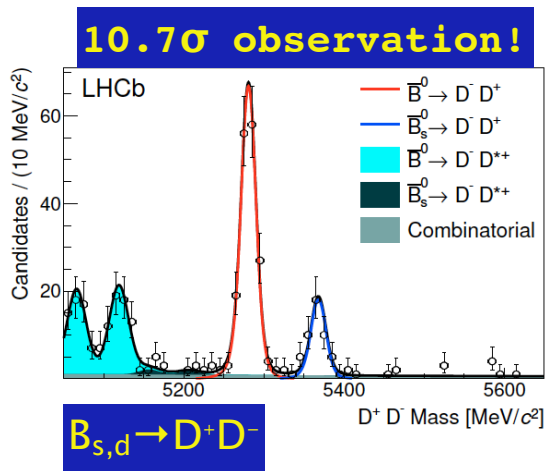


$$B_s \rightarrow D_s D^+$$

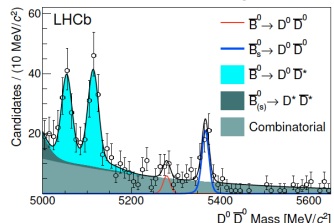
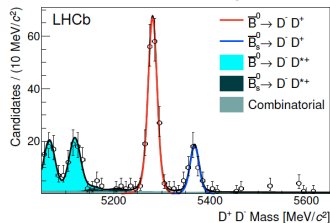
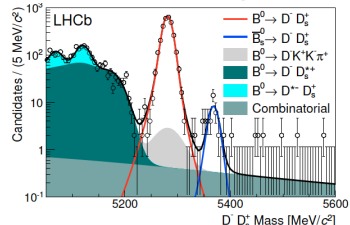
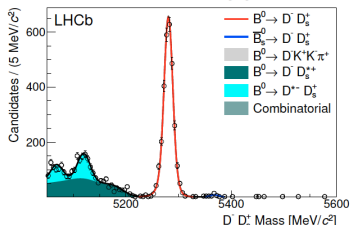
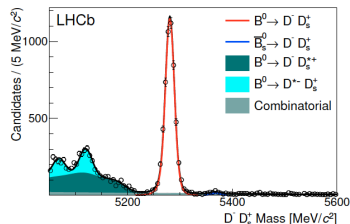
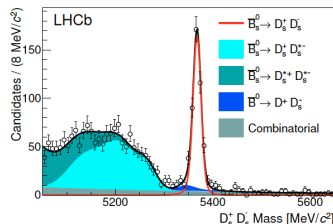
10 σ observation!



$$B_{d,s} \rightarrow D^+ D^-, D^0 D^0$$



Measured branching fractions



First observations of $B_s \rightarrow D_s D$, $D^+ D^-$, $D^0 D^0$
A strong hint for $B^0 \rightarrow D^0 D^0$

$$\frac{\mathcal{B}(\bar{B}_s^0 \rightarrow D^+ D^-)}{\mathcal{B}(\bar{B}^0 \rightarrow D^+ D^-)} = 1.08 \pm 0.20 \text{ (stat)} \pm 0.10 \text{ (syst)},$$

$$\frac{\mathcal{B}(\bar{B}_s^0 \rightarrow D_s^+ D^-)}{\mathcal{B}(B^0 \rightarrow D_s^+ D^-)} = 0.048 \pm 0.008 \text{ (stat)} \pm 0.004 \text{ (syst)},$$

$$\frac{\mathcal{B}(\bar{B}_s^0 \rightarrow D_s^+ D_s^-)}{\mathcal{B}(B^0 \rightarrow D_s^+ D_s^-)} = 0.55 \pm 0.03 \text{ (stat)} \pm 0.05 \text{ (syst)},$$

$$\frac{\mathcal{B}(\bar{B}_s^0 \rightarrow D^0 \bar{D}^0)}{\mathcal{B}(B^- \rightarrow D^0 D_s^-)} = 0.019 \pm 0.003 \text{ (stat)} \pm 0.003 \text{ (syst)},$$

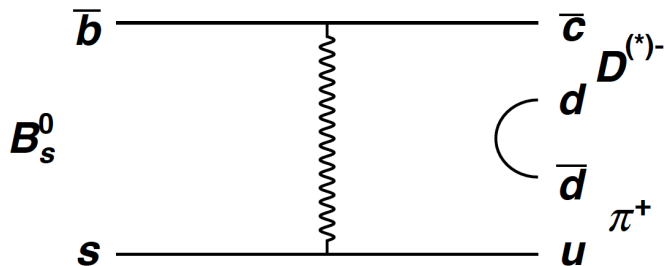
$$\frac{\mathcal{B}(\bar{B}^0 \rightarrow D^0 \bar{D}^0)}{\mathcal{B}(B^- \rightarrow D^0 D_s^-)} = 0.0014 \pm 0.0006 \text{ (stat)} \pm 0.0002 \text{ (syst)}$$

$$[< 0.0024 \text{ at } 90\% \text{ CL }],$$

$$\frac{\mathcal{B}(B^- \rightarrow D^0 D_s^-)}{\mathcal{B}(B^0 \rightarrow D_s^+ D^-)} = 1.20 \pm 0.02 \text{ (stat)} \pm 0.06 \text{ (syst)}.$$

BR results for $B_s \rightarrow D^+ D^-$, $D^0 D^0$ and $B^0 \rightarrow D^0 D^0$ at the upper end of rescattering predictions ([arXiv:1211.5785](https://arxiv.org/abs/1211.5785)).

Search for $B_s \rightarrow D^{*-} \pi^+$

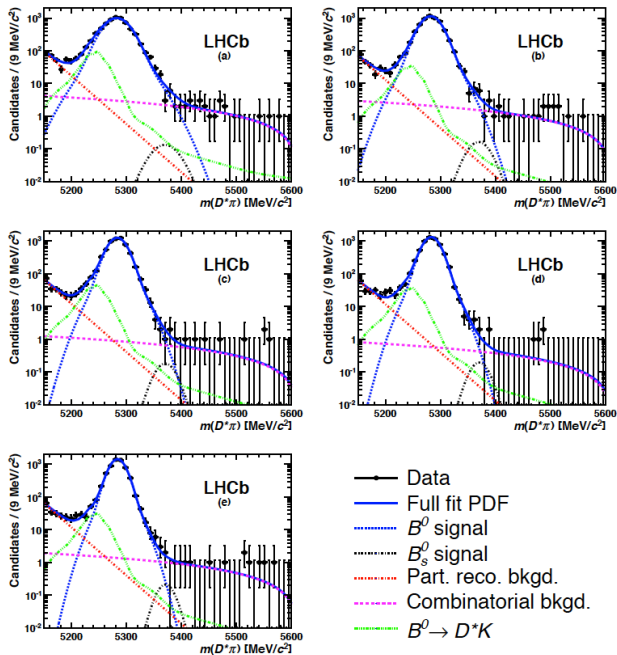


Pure weak exchange decay, helps to understand sizes of various diagrams and rescattering effects in DD decays.

Rescattering contributions to this decay are predicted to be small.

Interplay with other decays : e.g. if $BR(B_s \rightarrow \pi\pi)$ is driven by rescattering then expect small $BR(B_s \rightarrow D^* \pi)$. If $BR(B_s \rightarrow \pi\pi)$ is driven by short-distance effects then $BR(B_s \rightarrow D^* \pi)$ could be much larger.

Search for $B_s \rightarrow D^{*-} \pi^+$



Signal is divided into five bins based on the opening angle between the D^* and π momenta in the lab frame

Binning chosen to give equal numbers of events in each bin

Width of signal peak in highest bin 60% of that in lowest bin, sensitivity increased by 20%.

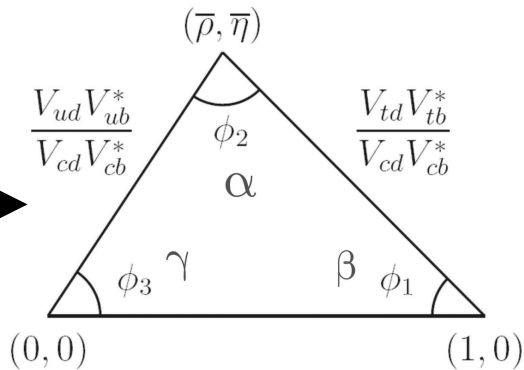
No signal found, Bayesian limit set

$BR(B_s \rightarrow D^* \pi) < 6.1(7.8) \cdot 10^{-6}$ at 90%(95%) CL

Suggestive of dominance of rescattering in $BR(B_s \rightarrow \pi \pi)$ as recently suggested in e.g. Gronau et al. ([arXiv:1211.5785](https://arxiv.org/abs/1211.5785)).

A measurement of the CKM angle γ

$$\begin{pmatrix} d' \\ s' \\ b' \end{pmatrix} = \begin{pmatrix} V_{ud} & V_{us} & V_{ub} \\ V_{cd} & V_{cs} & V_{cb} \\ V_{td} & V_{ts} & V_{tb} \end{pmatrix} \begin{pmatrix} d \\ s \\ b \end{pmatrix} = V_{CKM} \begin{pmatrix} d \\ s \\ b \end{pmatrix}$$



γ measurement inputs

GLW/ADS in $B \rightarrow DK, D\pi$ with $D \rightarrow hh$
ADS in $B \rightarrow DK, D\pi$ with $D \rightarrow hhhh$
GGSZ in $B \rightarrow DK$ with $D \rightarrow K_S hh$

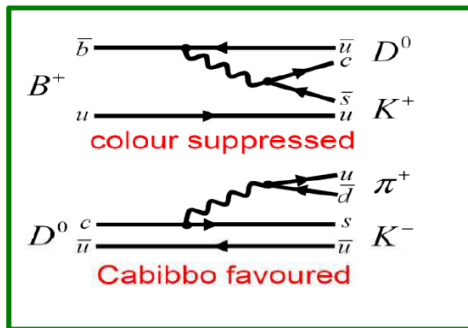
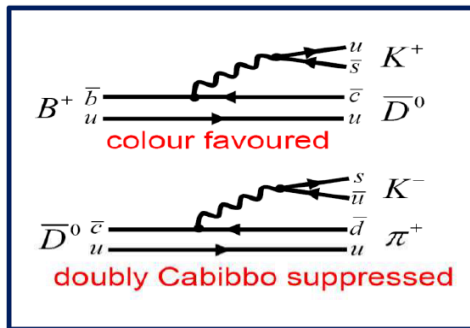
γ measurement inputs

GLW/ADS in $B \rightarrow DK, D\pi$ with $D \rightarrow hh$

ADS in $B \rightarrow DK, D\pi$ with $D \rightarrow hhhh$

GGSZ in $B \rightarrow DK$ with $D \rightarrow K_S hh$

Observables \Leftrightarrow physics parameters



GLW : D^0 decays to singly Cabibbo-suppressed final states ($KK, \pi\pi$), higher absolute yields but lower interference due to colour suppression

ADS : Combine colour-suppressed B decays with Cabibbo-favoured D decays in order to increase interference and hence sensitivity to γ

In both cases measure branching fractions and charge asymmetries

Same principle applies to $D\pi$ decays but interference smaller

Observables \Leftrightarrow physics parameters

r_B, δ_B are the amplitude ratio and relative strong phase of the interfering B decays

r_D, δ_D are hadronic parameters describing the $D^0 \rightarrow K\pi(\pi K)$ decays

r_D is the amplitude ratio of the CF to DCS D^0 decays

δ_D is the relative strong phase between the CF and DCS decays

Both are taken from CLEO measurements
([arXiv:0903.4853](https://arxiv.org/abs/0903.4853))

$$R_{K/\pi}^{K\pi} = R \frac{1 + (r_B r_D)^2 + 2r_B r_D \cos(\delta_B - \delta_D) \cos \gamma}{1 + (r_B^\pi r_D)^2 + 2r_B^\pi r_D \cos(\delta_B^\pi - \delta_D) \cos \gamma}$$

$$R_{K/\pi}^{KK} = R_{K/\pi}^{\pi\pi} = R \frac{1 + r_B^2 + 2r_B \cos \delta_B \cos \gamma}{1 + r_B^\pi{}^2 + 2r_B^\pi \cos \delta_B^\pi \cos \gamma}$$

$$A^{Fav} = \frac{2r_B r_D \sin(\delta_B - \delta_D) \sin \gamma}{1 + (r_B r_D)^2 + r_B r_D \cos(\delta_B - \delta_D) \cos \gamma}$$

$$A_\pi^{Fav} = \frac{2r_B^\pi r_D \sin(\delta_B^\pi - \delta_D) \sin \gamma}{1 + (r_B^\pi r_D)^2 + r_B^\pi r_D \cos(\delta_B^\pi - \delta_D) \cos \gamma}$$

$$A^{KK} = A^{\pi\pi} = \frac{2r_B \sin \delta_B \sin \gamma}{1 + r_B^2 + r_B \cos \delta_B \cos \gamma}$$

$$A_\pi^{KK} = A_\pi^{\pi\pi} = \frac{2r_B^\pi \sin \delta_B^\pi \sin \gamma}{1 + r_B^\pi{}^2 + r_B^\pi \cos \delta_B^\pi \cos \gamma}$$

$$R^{ADS} = \frac{r_B^2 + r_D^2 + 2r_B r_D \cos(\delta_B + \delta_D) \cos \gamma}{1 + (r_B r_D)^2 + 2r_B r_D \cos(\delta_B - \delta_D) \cos \gamma}$$

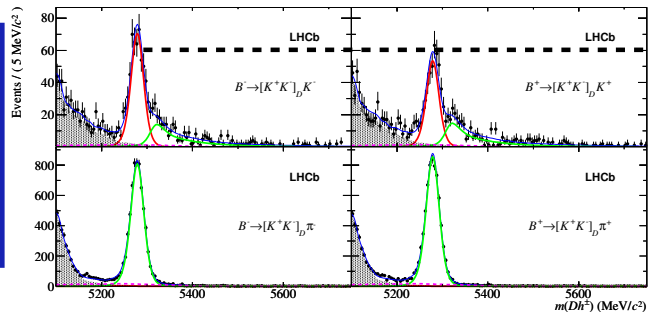
$$A^{ADS} = \frac{2r_B r_D \sin(\delta_B + \delta_D) \sin \gamma}{r_B^2 + r_D^2 + 2r_B r_D \cos(\delta_B + \delta_D) \cos \gamma}$$

$$R_\pi^{ADS} = \frac{r_B^\pi{}^2 + r_D^2 + 2r_B^\pi r_D \cos(\delta_B^\pi + \delta_D) \cos \gamma}{1 + (r_B^\pi r_D)^2 + 2r_B^\pi r_D \cos(\delta_B^\pi - \delta_D) \cos \gamma}$$

$$A_\pi^{ADS} = \frac{2r_B^\pi r_D \sin(\delta_B^\pi + \delta_D) \sin \gamma}{r_B^\pi{}^2 + r_D^2 + 2r_B^\pi r_D \cos(\delta_B^\pi + \delta_D) \cos \gamma}$$

Two body GLW signals

GLW, $D \rightarrow KK$



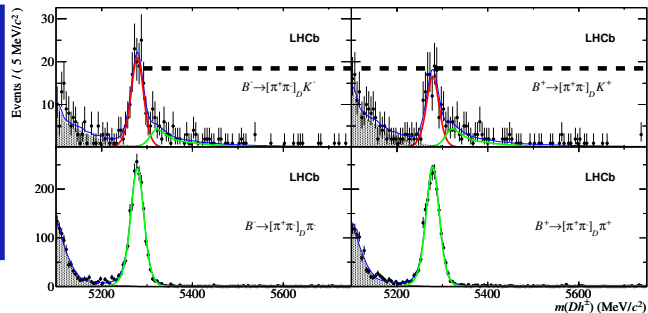
KK and $\pi\pi$ show similar-sized CP asymmetries, in the same direction

$$A_{CP+} = \langle A_K^{KK}, A_K^{\pi\pi} \rangle = 0.145 \pm 0.032 \pm 0.010$$

Branching fraction ratios consistent with CF D^0 decay mode

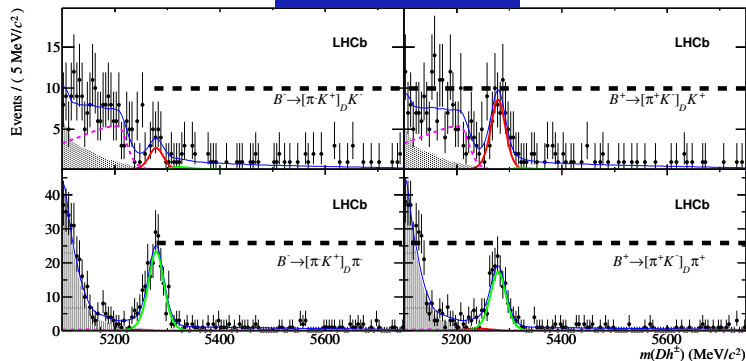
$$R_{CP+} = \frac{\langle R_{K/\pi}^{KK}, R_{K/\pi}^{\pi\pi} \rangle}{R_{K/\pi}^{K\pi}} = 1.007 \pm 0.038 \pm 0.012$$

GLW, $D \rightarrow \pi\pi$



Two body ADS signals

ADS, $D \rightarrow K\pi$



The Kaon mode shows a large CP asymmetry

$$A_{ADS(K)} = \frac{R_K^- - R_K^+}{R_K^- + R_K^+} = -0.520 \pm 0.150 \pm 0.021$$

And there is also a hint of something in the pion mode!

$$A_{ADS(\pi)} = \frac{R_\pi^- - R_\pi^+}{R_\pi^- + R_\pi^+} = 0.1426 \pm 0.0621 \pm 0.0110$$

ADS modes established at $>5\sigma$ significance

Combining all two body modes, direct CPV is observed at 5.8σ significance

γ measurement inputs

GLW/ADS in $B \rightarrow DK, D\pi$ with $D \rightarrow hh$

ADS in $B \rightarrow DK, D\pi$ with $D \rightarrow hhhh$

GGSZ in $B \rightarrow DK$ with $D \rightarrow K_S hh$

Observables \Leftrightarrow physics parameters

$$\Gamma(B^\pm \rightarrow D(K^\pm \pi^\mp \pi^+ \pi^-)K^\pm) \propto 1 + (r_B r_D^{K3\pi})^2 + 2\boxed{R_{K3\pi}} r_B r_D^{K3\pi} \cos(\delta_B - \delta_D^{K3\pi} \pm \gamma),$$

$$\Gamma(B^\pm \rightarrow D(K^\mp \pi^\pm \pi^+ \pi^-)K^\pm) \propto r_B^2 + (r_D^{K3\pi})^2 + 2\boxed{R_{K3\pi}} r_B r_D^{K3\pi} \cos(\delta_B + \delta_D^{K3\pi} \pm \gamma),$$

Same formalism as for the two-body case, except for the coherence factor $R_{K3\pi}$. This is necessary because the D^0 decay is a sum of amplitudes varying across the Dalitz plot; when we perform an analysis integrating over these amplitudes, we lose some sensitivity because of the way in which the decay interfere.

$R_{K3\pi}$ has been measured at CLEO and is small (~ 0.33) which indicates that these modes have a smaller sensitivity to γ when treated in this integrated manner than the two-body modes. However, they can still provide a good constraint on r_B .

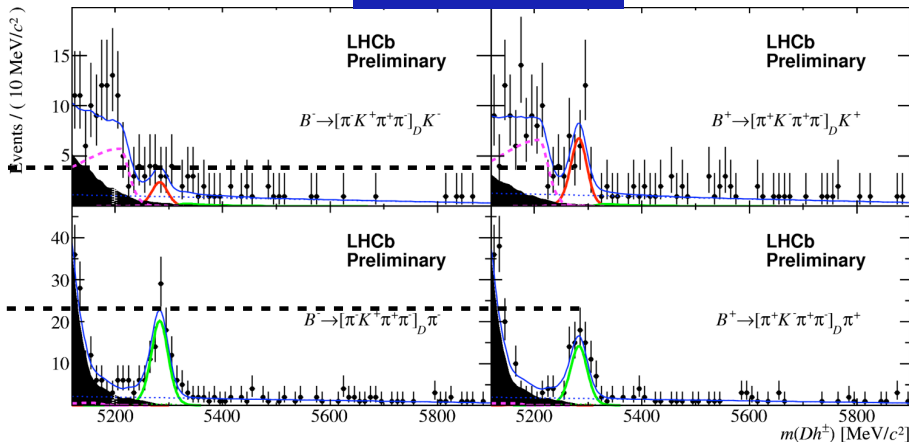
Four body ADS signals

ADS, $D \rightarrow K3\pi$

Once again, indications of CP asymmetries in both the Kaon and the Pion modes, going in the same direction as for the two-body modes.

$$A_{\text{ADS}(K)}^{K3\pi} = (R_K^{K3\pi,-} - R_K^{K3\pi,+}) / (R_K^{K3\pi,-} + R_K^{K3\pi,+}) = -0.42 \pm 0.22$$

$$A_{\text{ADS}(\pi)}^{K3\pi} = (R_\pi^{K3\pi,-} - R_\pi^{K3\pi,+}) / (R_\pi^{K3\pi,-} + R_\pi^{K3\pi,+}) = +0.13 \pm 0.10,$$



ADS modes established at $>5\sigma$ significance!

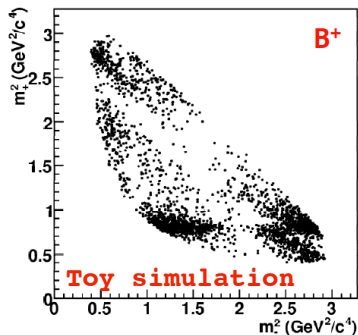
Gamma combination inputs

GLW/ADS in $B \rightarrow DK, D\pi$ with $D \rightarrow hh$

ADS in $B \rightarrow DK, D\pi$ with $D \rightarrow hhhh$

GGSZ in $B \rightarrow DK$ with $D \rightarrow K_s hh$

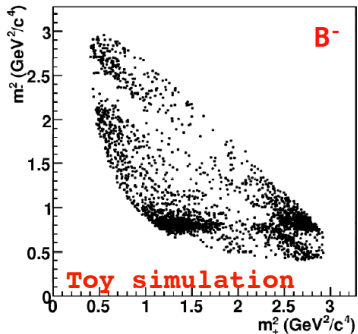
Observables \Leftrightarrow physics parameters



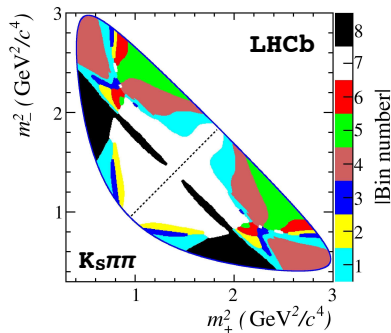
Here the decay chain is $B \rightarrow D^0 K$, with $D^0 \rightarrow K_S \pi \pi / K_S K K$

The D^0 decays proceed through many interfering amplitudes, some of which are Cabbibo-favoured, some singly Cabbibo-suppressed, and some doubly Cabbibo-suppressed

You are effectively doing a simultaneous ADS/GLW analysis, as long as you understand how the amplitudes and their phases vary across the Dalitz plot.



Observables \Leftrightarrow physics parameters



Here the decay chain is $B \rightarrow D^0 K$, with $D^0 \rightarrow K_S \pi \pi / K_S K K$

The D^0 decays proceed through many interfering amplitudes, some of which are Cabbibo-favoured, some singly Cabbibo-suppressed, and some doubly Cabbibo-suppressed

You are effectively doing a simultaneous ADS/GLW analysis, as long as you understand how the amplitudes and their phases vary across the Dalitz plot.

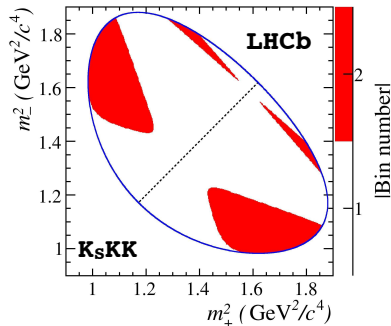
“Model-independent” : Bin the Dalitz plot and fit for yield of B^+ and B^- in each bin of the Dalitz plot, plugging in the strong phase in each bin from a CLEO measurement.

$$N_{+i}^+ = n_{B^+} [K_{-i} + (x_+^2 + y_+^2) K_{+i} + 2\sqrt{K_{+i} K_{-i}} (x_+ c_{+i} - y_+ s_{+i})]$$

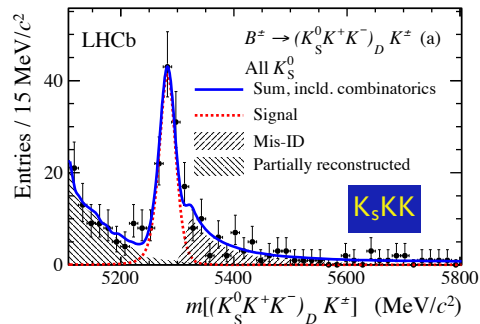
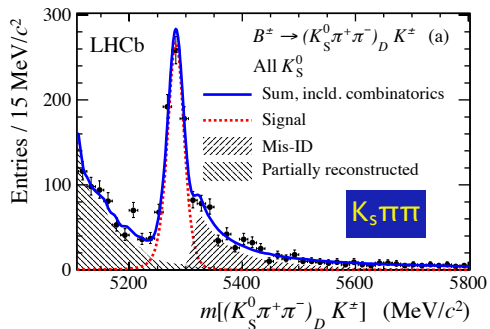
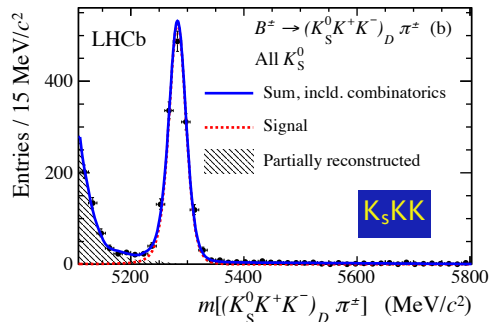
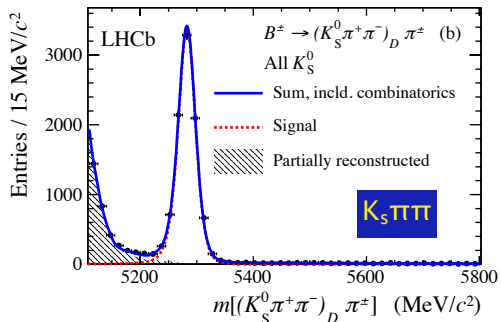
$$x_{\pm} = r_B \cos(\delta_B \pm \gamma), y_{\pm} = r_B \sin(\delta_B \pm \gamma)$$

c_i, s_i are the CLEO inputs

K_i are the yields of tagged D^0 decays in each bin

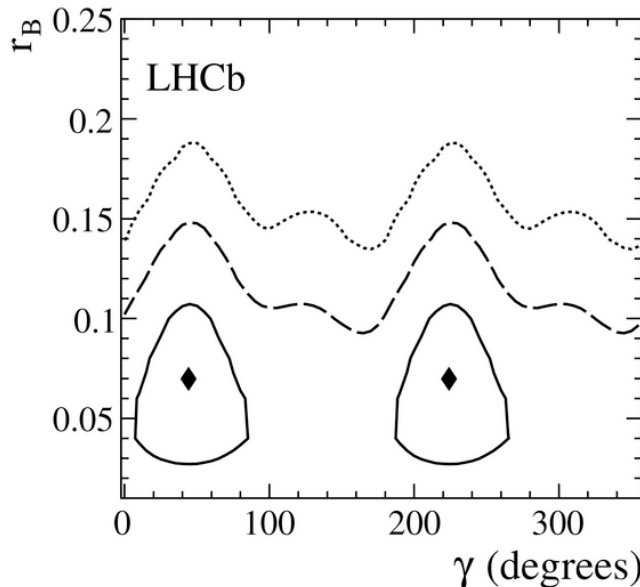
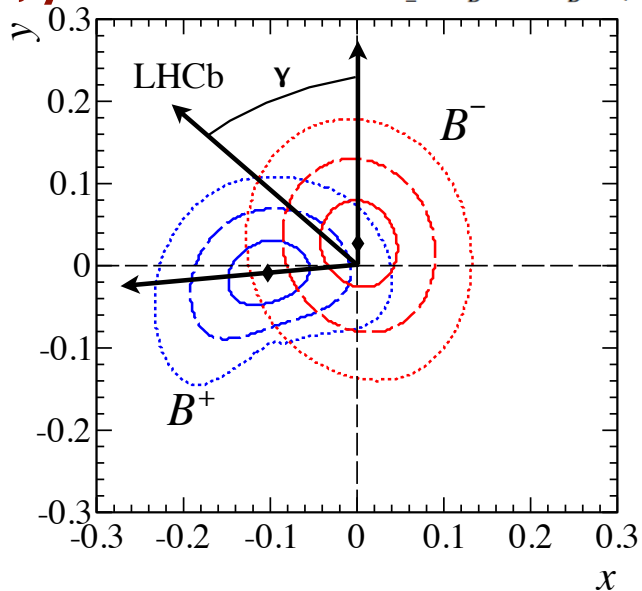


$K_S \pi \pi$ and $K_S K K$ signals



x^\pm, y^\pm

$$x_\pm = r_B \cos(\delta_B \pm \gamma), y_\pm = r_B \sin(\delta_B \pm \gamma)$$



Largest systematic arises from the assumption of no CPV in the control mode $D\pi$

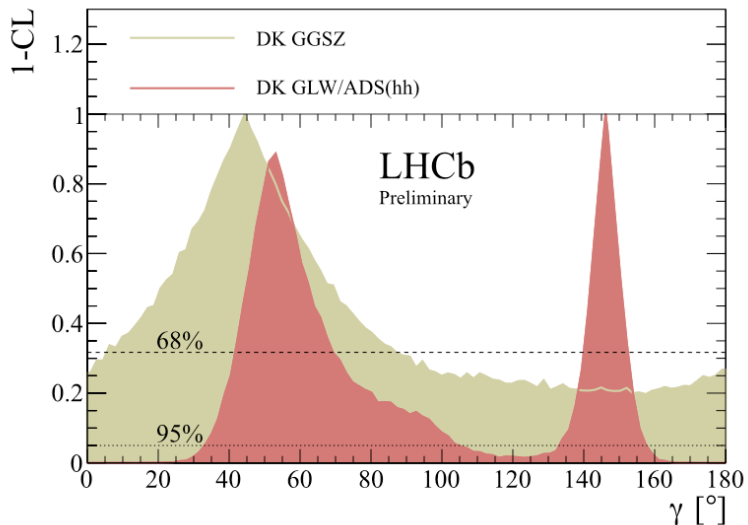
Little stand-alone sensitivity due to "unlucky" fluctuation of r_B

Putting it all
together

The LHCb γ combination

Look at ADS/GLW and GGSZ separately

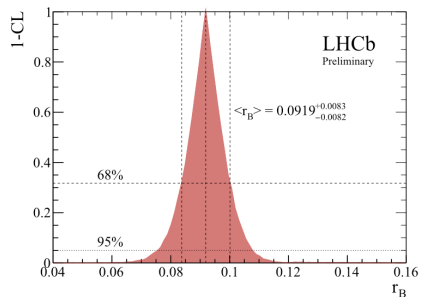
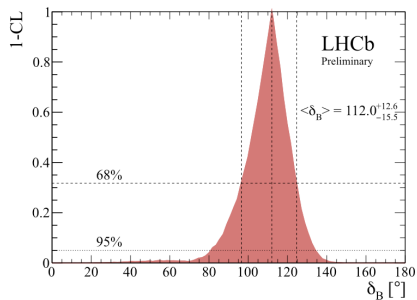
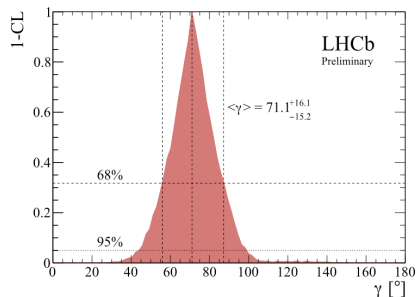
GGSZ has a poor standalone sensitivity because of an unlucky value of r_B .



The LHCb γ combination, DK only

Now combine all DK measurements, including $D \rightarrow K3\pi$ ADS

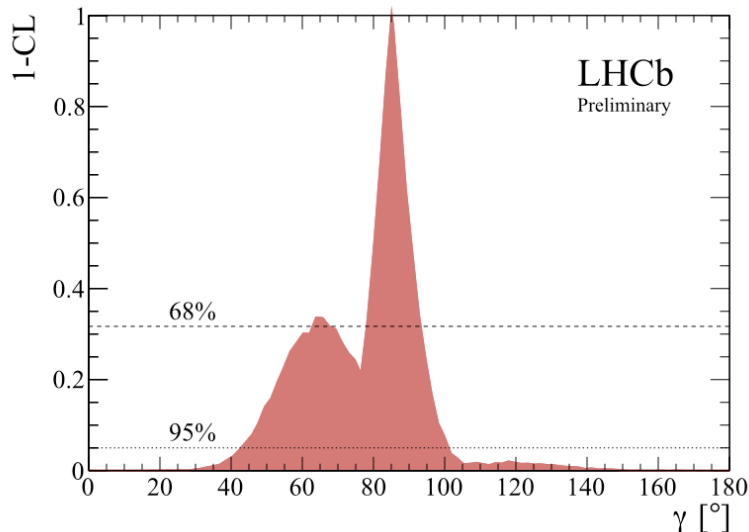
Rather Gaussian behaviour!



The LHCb γ combination, $DK+D\pi$

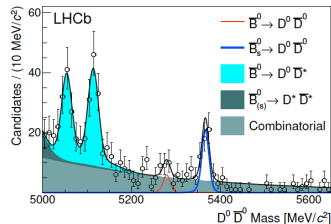
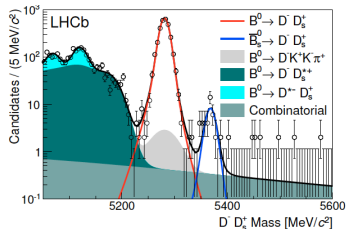
Now combine all DK measurements, including $D \rightarrow K3\pi$ ADS, and add $D\pi$ observables as well for the first time (details in the backups).

A second solution emerges at 1 sigma but 2 sigma intervals stable.



γ	63.7°	85.1°
68% CL	[61.8, 67.8]°	[77.9, 92.4]°
95% CL	← [43.8, 101.5]° →	
$r_{B(K)}$	0.0948	
68% CL	[0.0860, 0.1032]	
95% CL	[0.078, 0.111]	
$\delta_{B(K)}$	119.0°	
68% CL	[107.0, 129.1]°	
95% CL	[79.7, 137.9]°	
$r_{B(\pi)}$	0.0239	
68% CL	[0.0153, 0.0310]	
95% CL	[0.0, 0.037]	
$\delta_{B(\pi)}$	373.7°	321.4°
68% CL	[365.7, 387.0]°	[311.2, 328.4]°
95% CL	← [160.5, 333.6]° →	

Summary



The superb performance of the LHCb spectrometer is yielding a rich harvest of results in hadronic B decay modes

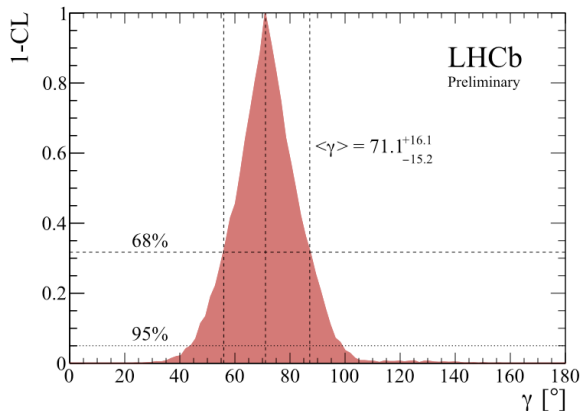
First observations of more and more suppressed decay modes

The combined measurement of the CKM angle γ with 1 fb^{-1} of data is as precise as the individual full dataset B factory measurements

And we have $>3 \text{ fb}$ on tape...

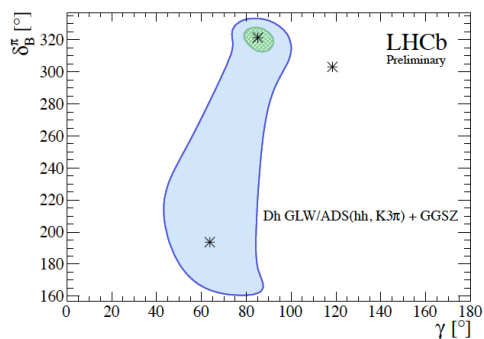
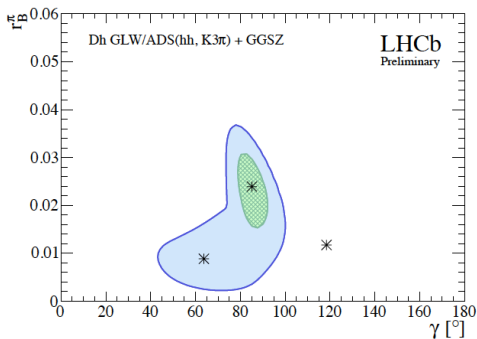
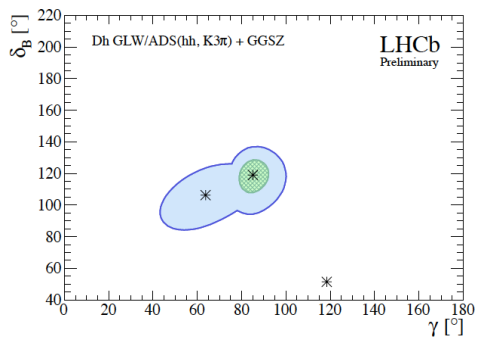
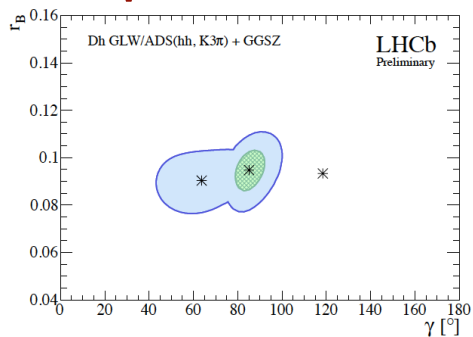
First measurements with the full 2011+2012 data are coming very soon; stay tuned!

Many thanks to the organizers for the invitation!



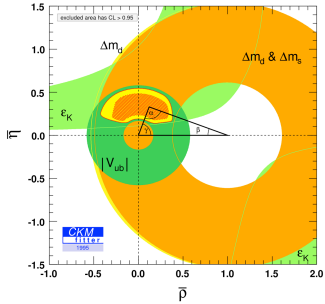
Backups

The LHCb γ combination, $DK+D\pi$

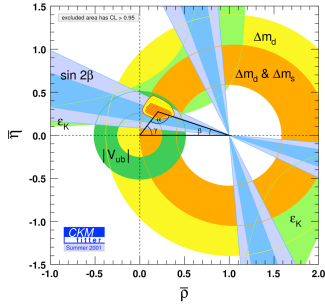


CKM triangle history

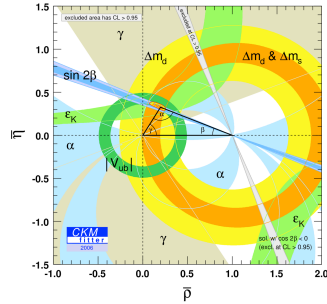
1995



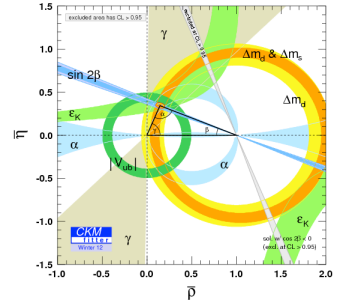
2001



2006



2012



Why γ ?

It is still probably the theoretically cleanest CKM parameter

We first review the methods for determining γ from $B \rightarrow DK$ decays that appeared after CKM 2008. We then discuss the theoretical errors in γ extraction. The errors due to neglected $D-\bar{D}$ and $B_{d,s}-\bar{B}_{d,s}$ mixing can be avoided by including their effects in the fits. The ultimate theoretical error is then given by electroweak corrections that we estimate to give a shift $\delta\gamma/\gamma \sim \mathcal{O}(10^{-6})$.

zupan, <http://arxiv.org/pdf/1101.0134.pdf>

Why γ ?

It is still probably the theoretically cleanest CKM parameter

Probe	Λ_{NP} for (N)MFV NP	Λ_{NP} for gen. FV NP	$B\bar{B}$ pairs
γ from $B \rightarrow DK^{1)}$	$\Lambda \sim \mathcal{O}(10^2 \text{ TeV})$	$\Lambda \sim \mathcal{O}(10^3 \text{ TeV})$	$\sim 10^{18}$
$B \rightarrow \tau\nu^{2)}$	$\Lambda \sim \mathcal{O}(\text{ TeV})$	$\Lambda \sim \mathcal{O}(30 \text{ TeV})$	$\sim 10^{13}$
$b \rightarrow ssd^{3)}$	$\Lambda \sim \mathcal{O}(\text{ TeV})$	$\Lambda \sim \mathcal{O}(10^3 \text{ TeV})$	$\sim 10^{13}$
β from $B \rightarrow J/\psi K_S^{4)}$	$\Lambda \sim \mathcal{O}(50 \text{ TeV})$	$\Lambda \sim \mathcal{O}(200 \text{ TeV})$	$\sim 10^{12}$
$K - \bar{K}$ mixing ⁵⁾	$\Lambda > 0.4 \text{ TeV}$ (6 TeV)	$\Lambda > 10^{3(4)} \text{ TeV}$	now

Table 1: *The ultimate NP scales that can be probed using different observables listed in the first column. They are given by saturating the theoretical errors given respectively by 1) $\delta\gamma/\gamma = 10^{-6}$, 2) optimistically assuming no error on f_B , so that ultimate theoretical error just from electroweak corrections, 3) using SM predictions in [20], 4) optimistically assuming perturbative error estimates $\delta\beta/\beta$ 0.1% [21], and 5) from bounds for $\text{Re}C_1(\text{Im}C_1)$ from UTfitter [23].*

zupan, <http://arxiv.org/pdf/1101.0134.pdf>

BABAR γ , CKM

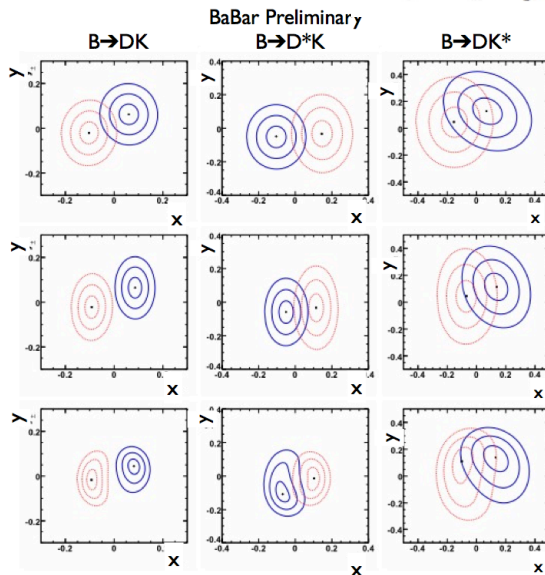
BABAR : combination in Cartesian coordinates

$$\gamma = (69_{-16}^{+17})^\circ$$

GGSZ

GGSZ+GLW

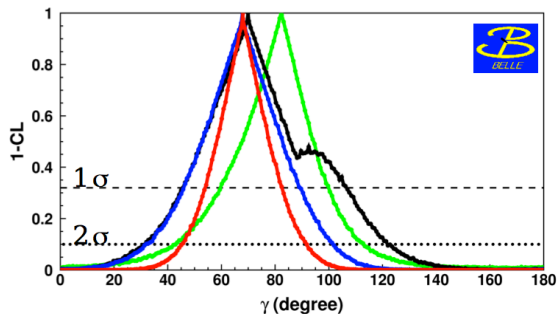
GGSZ+GLW+ADS



The improvement is clearly visible.

BELLE γ , CKM

BELLE : projections in γ , r_B



GGSZ

$$\gamma = [82^{+18}_{-23}]^\circ$$

GGSZ+ADS

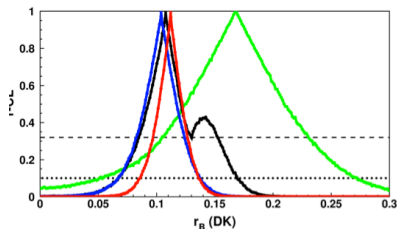
$$\gamma = [70^{+37}_{-24}]^\circ$$

GGSZ+ADS+ δ_D

$$\gamma = [68 \pm 22]^\circ$$

GGSZ+ADS+GLW+ δ_D

$$\gamma = [68^{+15}_{-14}]^\circ$$



for $B \rightarrow DK$:

$$(2\sigma = {}^{+28^\circ}_{-27})$$

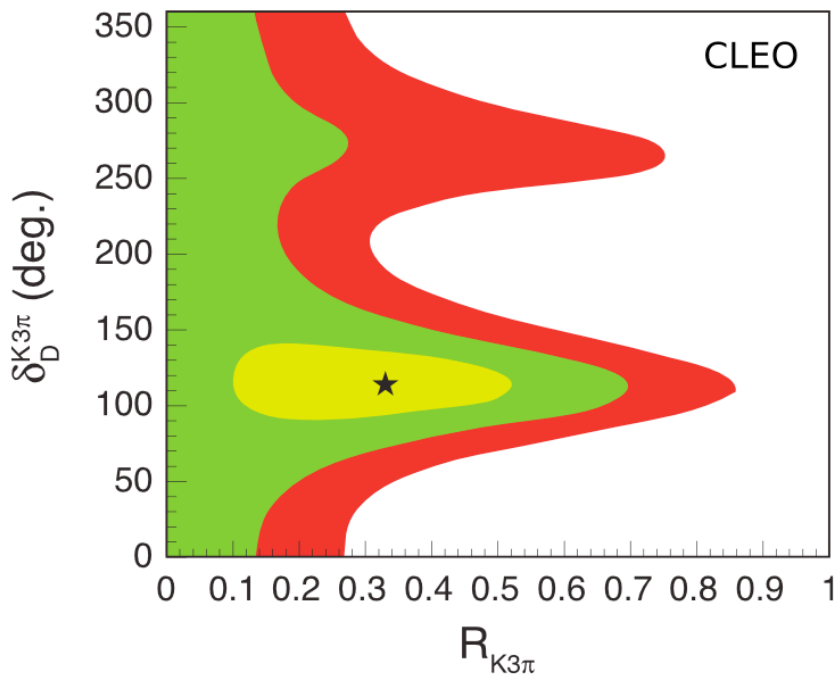
$$r_B = 0.168^{+0.063}_{-0.064}$$

$$r_B = 0.108^{+0.045}_{-0.023}$$

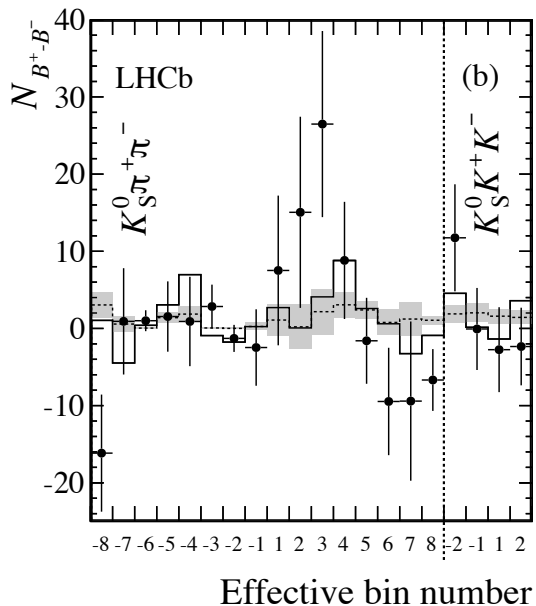
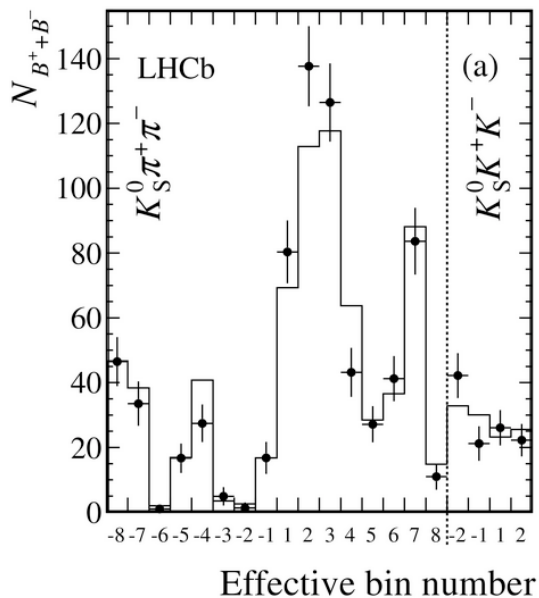
$$r_B = 0.104^{+0.020}_{-0.021}$$

$$\mathbf{r_B = 0.112^{+0.014}_{-0.015}}$$

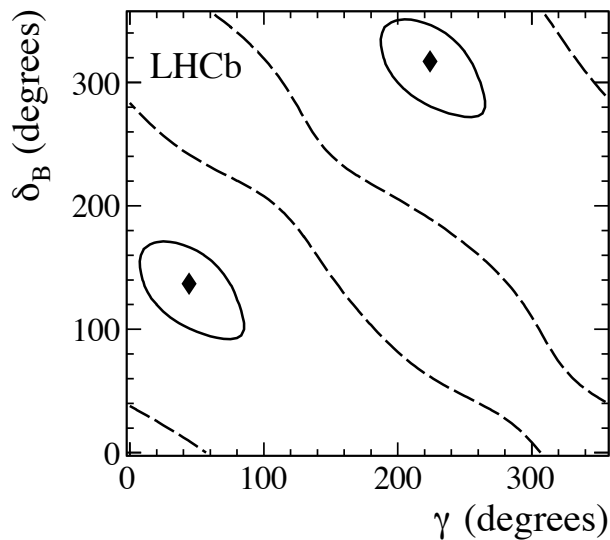
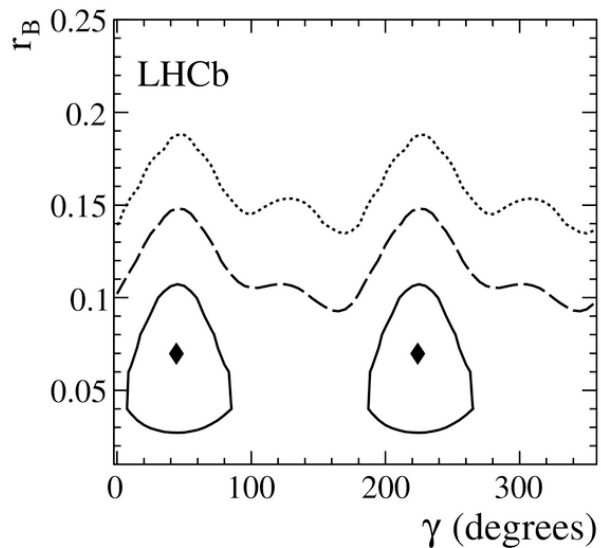
CLEO inputs



GGSZ asymmetries per bin



GGSZ only extractions



GLW/ADS full results

$$\begin{aligned}
R_{K/\pi}^{K\pi} &= 0.0774 \pm 0.0012 \pm 0.0018 \\
R_{K/\pi}^{KK} &= 0.0773 \pm 0.0030 \pm 0.0018 \\
R_{K/\pi}^{\pi\pi} &= 0.0803 \pm 0.0056 \pm 0.0017 \\
A_{\pi}^{K\pi} &= -0.0001 \pm 0.0036 \pm 0.0095 \\
A_K^{K\pi} &= 0.0044 \pm 0.0144 \pm 0.0174 \\
A_K^{KK} &= 0.148 \pm 0.037 \pm 0.010 \\
A_K^{\pi\pi} &= 0.135 \pm 0.066 \pm 0.010 \\
A_{\pi}^{KK} &= -0.020 \pm 0.009 \pm 0.012 \\
A_{\pi}^{\pi\pi} &= -0.001 \pm 0.017 \pm 0.010 \\
R_K^{-} &= 0.0073 \pm 0.0023 \pm 0.0004 \\
R_K^{+} &= 0.0232 \pm 0.0034 \pm 0.0007 \\
R_{\pi}^{-} &= 0.00469 \pm 0.00038 \pm 0.00008 \\
R_{\pi}^{+} &= 0.00352 \pm 0.00033 \pm 0.00007.
\end{aligned}$$

Table 2: Systematic uncertainties on the observables. PID refers to the fixed efficiency of the $DLL_{K\pi}$ cut on the bachelor track. PDFs refers to the variations of the fixed shapes in the fit. “Sim” refers to the use of simulation to estimate relative efficiencies of the signal modes which includes the branching fraction estimates of the Λ_b^0 background. $A_{\text{instr.}}$ quantifies the uncertainty on the production, interaction and detection asymmetries.

$\times 10^{-3}$	PID	PDFs	Sim	$A_{\text{instr.}}$	Total
$R_{K/\pi}^{K\pi}$	1.4	0.9	0.8	0	1.8
$R_{K/\pi}^{KK}$	1.3	0.8	0.9	0	1.8
$R_{K/\pi}^{\pi\pi}$	1.3	0.6	0.8	0	1.7
$A_{\pi}^{K\pi}$	0	1.0	0	9.4	9.5
$A_K^{K\pi}$	0.2	4.1	0	16.9	17.4
A_K^{KK}	1.6	1.3	0.5	9.5	9.7
$A_{\pi}^{\pi\pi}$	1.9	2.3	0	9.0	9.5
$A_K^{\pi\pi}$	0.1	6.6	0	9.5	11.6
R_K^{-}	0.1	0.4	0	9.9	9.9
R_K^{+}	0.2	0.4	0	0.1	0.4
R_{π}^{-}	0.4	0.5	0	0.1	0.7
R_{π}^{+}	0.01	0.03	0	0.07	0.08
R_{π}^{+}	0.01	0.03	0	0.07	0.07

GLW/ADS 4h full results

Table 2: Systematic uncertainties on the observables. ‘PID’ refers to the fixed efficiency for the bachelor DLL_{Kπ} requirement which is determined using the D^{*+} calibration sample. ‘PDFs’ refers to the variations of the fixed shapes in the fit. ‘Sim’ refers to the use of simulation to estimate relative efficiencies of the signal modes. ‘ $A_{\text{instr.}}$ ’ quantifies the uncertainty on the production, interaction and detection asymmetries.

$[\times 10^{-3}]$	$R_{K/\pi}^{K3\pi}$	$A_{\pi}^{K3\pi}$	$A_K^{K3\pi}$	$R_K^{K3\pi,-}$	$R_K^{K3\pi,+}$	$R_{\pi}^{K3\pi,-}$	$R_{\pi}^{K3\pi,+}$
PID	1.7	0.2	0.6	0.4	0.4	0.02	0.04
PDFs	1.2	1.3	4.4	0.7	0.9	0.09	0.08
Sim	1.5	0.1	0.3	0.1	0.2	0.01	0.02
$A_{\text{instr.}}$	0.0	9.9	17.1	0.1	0.1	0.06	0.06
Total	2.6	10.0	17.7	0.8	1.0	0.11	0.11

$$R_{K/\pi}^{K3\pi} = 0.0771 \pm 0.0017 \pm 0.0026$$

$$A_K^{K3\pi} = -0.029 \pm 0.020 \pm 0.018$$

$$A_{\pi}^{K3\pi} = -0.006 \pm 0.005 \pm 0.010$$

$$R_K^{K3\pi,-} = 0.0072 \pm_{-0.0032}^{+0.0036} \pm 0.0008$$

$$R_K^{K3\pi,+} = 0.0175 \pm_{-0.0039}^{+0.0043} \pm 0.0010$$

$$R_{\pi}^{K3\pi,-} = 0.00417 \pm_{-0.00050}^{+0.00054} \pm 0.00011$$

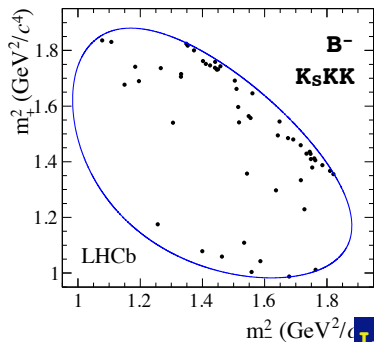
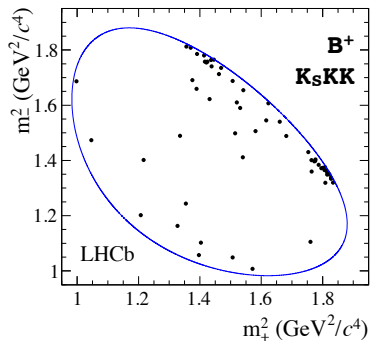
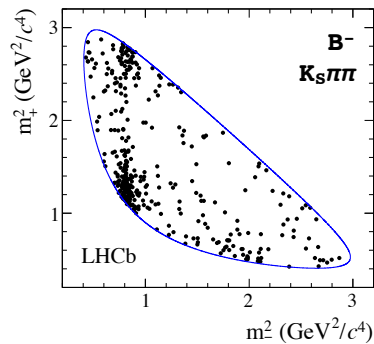
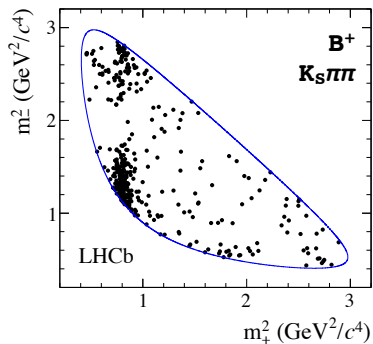
$$R_{\pi}^{K3\pi,+} = 0.00321 \pm_{-0.00045}^{+0.00048} \pm 0.00011$$

GGSZ full results

Table 3: Results for x_{\pm} and y_{\pm} from the fits to the data in the case when both $D \rightarrow K_s^0 \pi^+ \pi^-$ and $D \rightarrow K_s^0 K^+ K^-$ are considered and when only the $D \rightarrow K_s^0 \pi^+ \pi^-$ final state is included. The first, second, and third uncertainties are the statistical, the experimental systematic, and the error associated with the precision of the strong-phase parameters, respectively. The correlation coefficients are calculated including all sources of uncertainty (the values in parentheses correspond to the case where only the statistical uncertainties are considered).

Parameter	All data	$D \rightarrow K_s^0 \pi^+ \pi^-$ alone
$x_- [\times 10^{-2}]$	$0.0 \pm 4.3 \pm 1.5 \pm 0.6$	$1.6 \pm 4.8 \pm 1.4 \pm 0.8$
$y_- [\times 10^{-2}]$	$2.7 \pm 5.2 \pm 0.8 \pm 2.3$	$1.4 \pm 5.4 \pm 0.8 \pm 2.4$
$\text{corr}(x_-, y_-)$	$-0.10 (-0.11)$	$-0.12 (-0.12)$
$x_+ [\times 10^{-2}]$	$-10.3 \pm 4.5 \pm 1.8 \pm 1.4$	$-8.6 \pm 5.4 \pm 1.7 \pm 1.6$
$y_+ [\times 10^{-2}]$	$-0.9 \pm 3.7 \pm 0.8 \pm 3.0$	$-0.3 \pm 3.7 \pm 0.9 \pm 2.7$
$\text{corr}(x_+, y_+)$	$0.22 (0.17)$	$0.20 (0.17)$

Dalitz distributions for signal



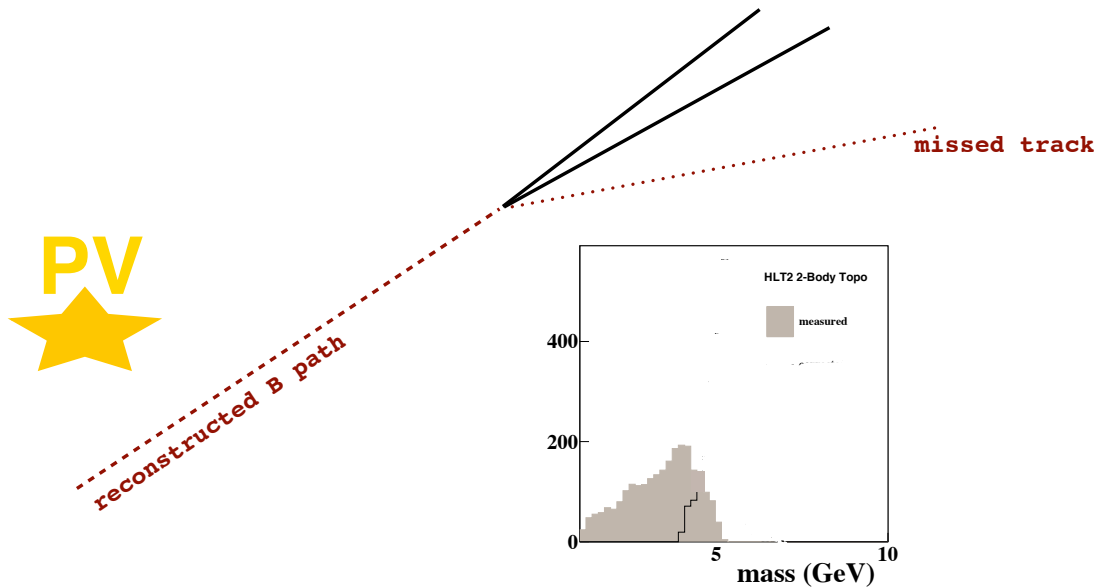
Multivariate selections from the start

Question : How is LHCb achieving clean signals in a much dirtier environment than either the B-factories or CDF?

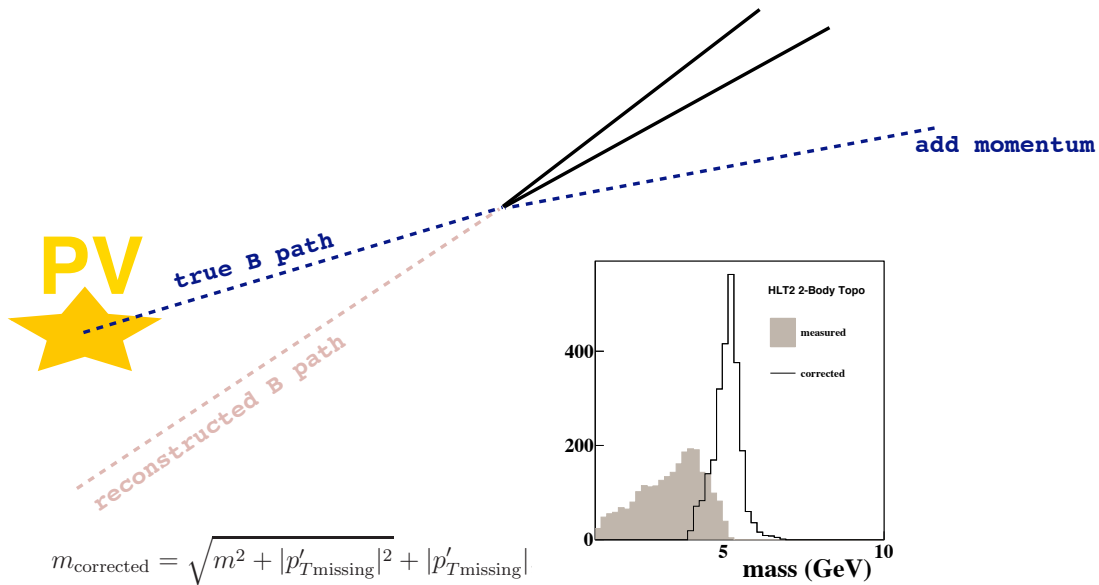
Answer 1 : A state of the art detector with $\sim 0.5\%$ momentum resolution and powerful particle identification.

Answer 2 : An aggressive use of multivariate selections from the very first stage of the data-taking process, the trigger.

A topological decision tree trigger

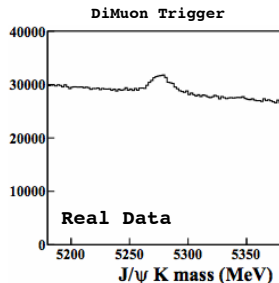
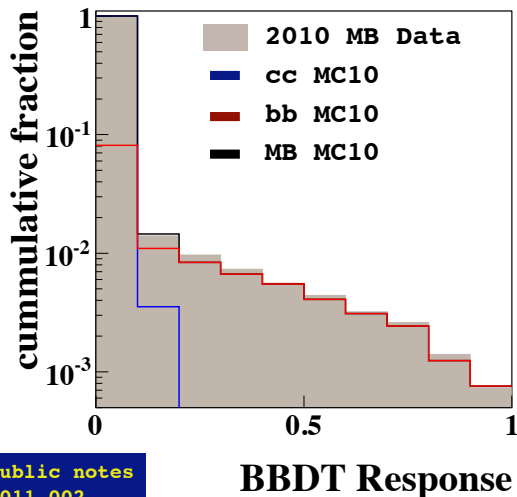


A topological decision tree trigger

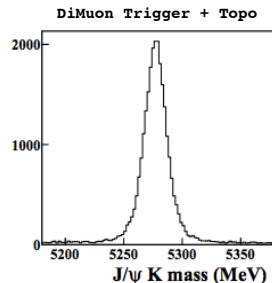


A topological decision tree trigger

The corrected mass is a good variable, but not good enough to deal with pileup on its own : deploy a boosted decision tree to discriminate between signal and background displaced vertices.



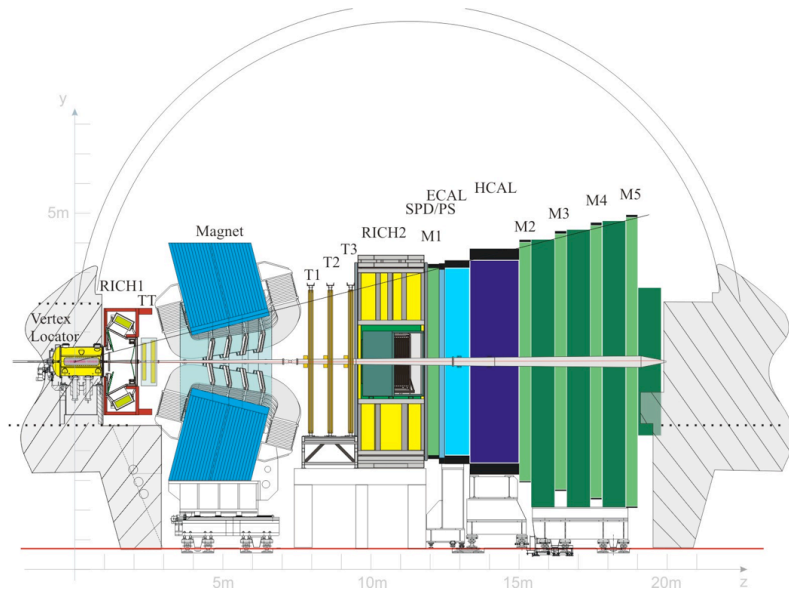
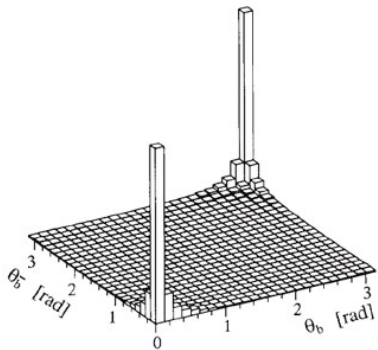
Left : $J/\psi K$ candidates with a dimuon trigger and no detachment required



Right : the subset of these candidates which pass the topological trigger

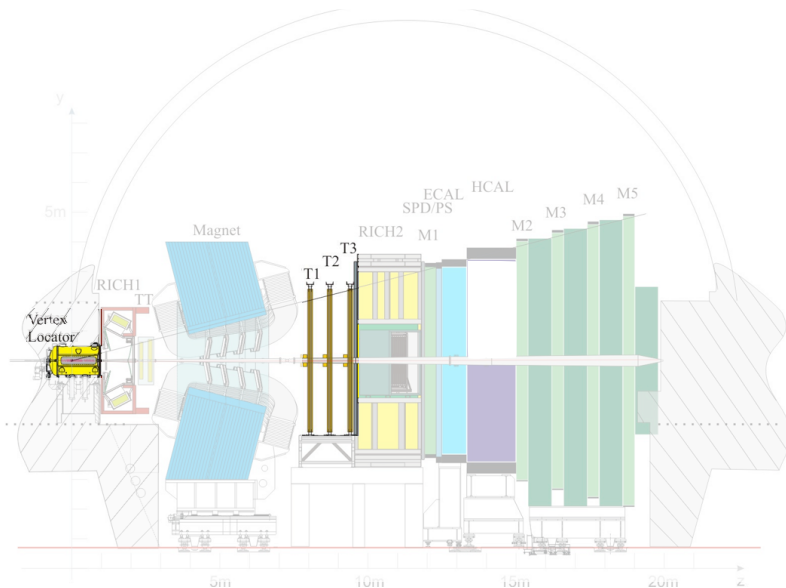
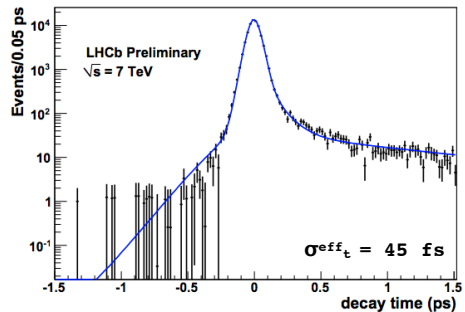
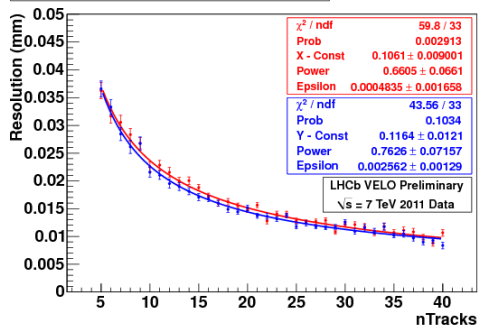
See LHCb public notes
LHCb-PUB-2011-002
LHCb-PUB-2011-003
LHCb-PUB-2011-016

The LHCb spectrometer



The LHCb spectrometer

X and Y resolution - offline, exactly 1 PV



The LHCb spectrometer

